Annales
Geophysicae

Semiannual and annual variations in the height of the ionospheric F2-peak

H. Rishbeth[1], **K. J. F. Sedgemore-Schulthess**[1], **T. Ulich**[2]

[1] Department of Physics and Astronomy, University of Southampton, Southampton SO17 1BJ, UK
[2] Sodankylä Geophysical Observatory, Tähteläntie 112, Sodankylä FIN-90570 Finland

Abstract. Ionosonde data from sixteen stations are used to study the semiannual and annual variations in the height of the ionospheric F2-peak, hmF2. The semiannual variation, which peaks shortly after equinox, has an amplitude of about 8 km at an average level of solar activity (10.7 cm flux = 140 units), both at noon and midnight. The annual variation has an amplitude of about 11 km at northern midlatitudes, peaking in early summer; and is larger at southern stations, where it peaks in late summer. Both annual and semiannual amplitudes increase with increasing solar activity by day, but not at night. The semiannual variation in hmF2 is unrelated to the semiannual variation of the peak electron density NmF2, and is not reproduced by the CTIP and TIME-GCM computational models of the quiet-day thermosphere and ionosphere. The semiannual variation in hmF2 is approximately "isobaric", in that its amplitude corresponds quite well to the semiannual variation in the height of fixed pressure-levels in the thermosphere, as represented by the MSIS empirical model. The annual variation is not "isobaric". The annual mean of hmF2 increases with solar 10.7 cm flux, both by night and by day, on average by about 0.45 km/flux unit, rather smaller than the corresponding increase of height of constant pressure-levels in the MSIS model. The discrepancy may be due to solar-cycle variations of thermospheric winds. Although geomagnetic activity, which affects thermospheric density and temperature and therefore hmF2 also, is greatest at the equinoxes, this seems to account for less than half the semiannual variation of hmF2. The rest may be due to a semiannual variation of tidal and wave energy transmitted to the thermosphere from lower levels in the atmosphere.

Key words: Atmospheric composition and structure (thermosphere – composition and chemistry) – Ionosphere (mid-latitude ionosphere)

Correspondence to: H. Rishbeth

1 Introduction

Several atmospheric, ionospheric and geomagnetic parameters display a regular semiannual (6-monthly) variation, with maxima near the March and September equinoxes. They include the peak electron density of the ionospheric F2-layer (NmF2) in some parts of the world (Burkard, 1951; Yonezawa and Arima, 1959; Chaman Lal, 1992); the height of the F2-layer peak (hmF2) (Becker, 1967); the neutral air density ρ in the thermosphere (Paetzold and Zschörner, 1961); and geomagnetic indices such as Kp and Ap (Bartels, 1963; Green, 1984). Semiannual oscillations also exist in the lower and middle atmosphere. Annual (12-monthly) variations also exist in hmF2 and ρ, with maxima usually in summer. The case of noon NmF2 is complicated: in some parts of the world its predominant variation is semiannual, but elsewhere it is annual, usually with a winter maximum (e.g. Yonezawa and Arima, 1959; Yonezawa, 1971; Torr and Torr, 1973).

Most of these annual and semiannual phenomena have been extensively studied. An exception is the semiannual variation in hmF2, which does not seem to have received much discussion since Becker's (1964, 1967) papers thirty years ago. Figure 1 shows the 27-day running mean of noon hmF2 for a twelve month period in 1963–1964 at Lindau, Germany, derived by real height N(h) analysis of ionograms by Becker (1967). The day-to-day variability of hmF2 has been considerably smoothed by the 27-day averaging (judging from Becker's daily values during this period which are shown in Fig. 5 of Rawer, 1969). Also plotted in Fig. 1 is the average month-by-month variation of the magnetic parameter Ap, which shows the equinox peaks in magnetic activity, the influence of which is discussed in Sect. 4.2 (the September peak is influenced by an immense storm, with Ap = 126 on 22 September, 1963). During these 12 months, the solar 10.7 cm radio flux $F_{10.7}$ (used as a conventional indicator of solar activity) was fairly steady, in the range 75–90 flux units, except in late
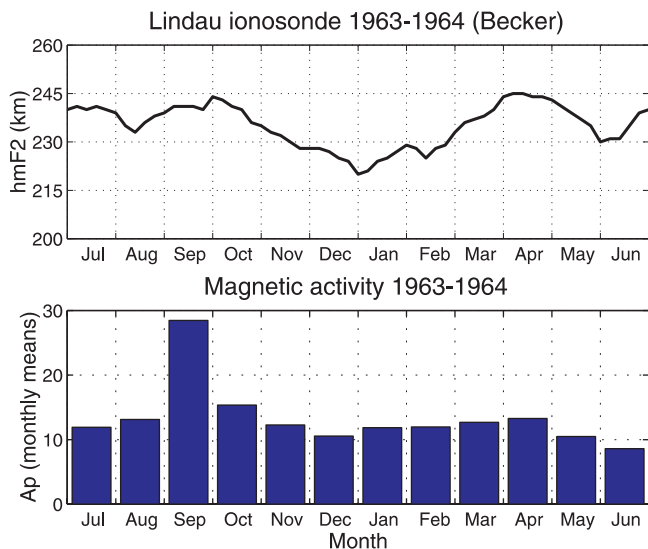
Fig. 1. Plot of hmF2 at Lindau (52°N), as derived from ionograms by Becker (1967), and the geomagnetic index Ap for the 12-month period July 1963 to June 1964

September 1963 when it rose to around 100 units. The semiannual variation is not so consistent or well-defined for the period 1957–1958. The dependence on $F_{10.7}$ of day-to-day values of hmF2 is not clear-cut, in that the Lindau data for 1958 show a great deal of scatter when plotted against $F_{10.7}$ (Becker, 1964). Eccles *et al.* (1967) commented on Becker's results, but they could only reproduce a semiannual variation of hmF2 by the device of imposing a semiannual temperature variation in their model.

Further investigation of hmF2 is required. Concentrating on midday and midnight, we tackle the question in two ways: in Sect. 2 by Fourier analysis of hmF2 data from several ionosonde stations over three solar cycles, and in Sect. 3 by using the global thermospheric models TIME-GCM (Roble *et al.*, 1988) and CTIP (Fuller-Rowell *et al.*, 1996; Millward *et al.*, 1996a). In Sect. 4 we investigate whether the variations of hmF2 are "isobaric", by comparing them with the variations in height of fixed pressure-levels in the thermosphere, as expressed by the MSISE-90 thermospheric model. We also estimate the effect on hmF2 of geomagnetic activity, in particular the equinoctial peaks in Ap. In Sect. 5 we review possible causes of the semiannual variation of hmF2.

2 Values of *h*mF2 derived from ionosonde data

2.1 Analysis

Our data comprise values of hmF2 for sixteen stations (Table 1a, b). The values of hmF2 were derived from "MUF factors" (M3000) tabulated in ionosonde data taken from the National Geophysical Data Centre Vertical Sounding Database, using the formulae proposed by Shimazaki (1955) and Bilitza *et al.* (1979). M3000 is the factor which, in theory, relates the maximum usable frequency for propagation over a 3000 km path to the ordinary critical frequency foF2. According to the "Shimazaki formula", which assumes the idealized case of radio waves reflected from a parabolic F2 layer above a spherical Earth:

$$h\text{mF2} = \{1490/M3000\} - 176 \text{ [km]} \tag{1a}$$

The "Bilitza formula", which allows for the effect of ionization below the F2-layer, takes the form

$$h\text{mF2} = \{1490/(M3000 + \Delta M(X))\} - 176 \text{ [km]} \tag{1b}$$

where $\Delta M(X)$ is an empirical function of the critical frequency ratio $X = f\text{oF2}/f\text{oE}$, taking account of sunspot number and geomagnetic latitude. The correction is important by day, as we show later, but is sufficiently small at night for the plain "Shimazaki formula" Eq. (1a) to be used. The formulas are unreliable if M3000 is small, i.e. the layer is high, or if foF2 is too close to foE (e.g. Dudeney, 1983). Ulich and Turunen (1997) find that the Bilitza formula overestimates daytime hmF2, on average by 18 km, as compared to the value found from real height inversion (using the polynomial method of Titheridge, 1969). As the error depends on X and increases when X is large (McNamara *et al.*, 1987), as at solar maximum, it may affect our results for the solar cycle variations of hmF2.

It is most desirable to use data that are consistently scaled and well-calibrated across any changes of instrument and site. Several stations that we used meet this criterion, but not necessarily for the whole period 1957–1994 spanned by our data. To increase confidence in the analysis, we imposed the conditions M3000 > 2.5 and X > 1.7, which limited the number of stations for which we had MUF data of acceptable quality, especially at night. Only a few stations in the Southern Hemisphere met the criteria, and we omitted stations near the magnetic equator, because of doubts about the reliability of any MUF-based formula. We use monthly medians, averaging the daytime values of hmF2 over the period 10–14 LT and the nighttime values over 22–02 LT. Our analysis program makes a linear interpolation through data gaps of up to three months while rejecting data containing longer gaps; for most stations, we have useful results for 25–30 years. As magnetic activity is enhanced at the equinoxes, the median values for equinox months correspond to higher levels of Ap than do those for solstice months; in Sect. 4.2 we discuss the possible effect of this on our results.

2.2 Annual means of hmF2

The month-by-month data for sixteen stations are shown in Fig. 2. At all these stations, hmF2 is clearly higher at night than by day, and the day and night plots clash only at Kerguelen. Perusal of the plots shows an overlying solar-cycle variation everywhere, with marked station-to-station differences in annual and semiannual variations. For example, by day the annual variations are especially strong at Port Stanley, and at Moscow the semiannual variation has noticeably higher peaks in

Table 1. a Height hmF2 at midday (10–14 LT) for solar flux $F_{10.7}$ = 140 units, computed from ionosonde "MUF" data; h_0 is the annual mean, h'_0 is the rate of change $dh_0/dF_{10.7}$; the amplitudes h_1 and h_2 refer to the annual and semiannual components as defined in Eq. (2). Stations are arranged in order of magnetic invariant latitude. **b.** Height hmF2 at night (22-02 LT) for solar flux $F_{10.7}$ = 140 units, computed from ionosonde "MUF" data. Layout as for Table 1a

| Station	Geographic latitude (°)	Geographic longitude (°)	Magnetic latitude (°)	Annual mean		Amplitudes		Phases	
				h_0 (km)	h'_0 (km/unit)	h_1 (km)	h_2 (km)	ϕ_1 (mo)	ϕ_2 (mo)
a									
1. Kiruna	68N	20E	+65	265		10.5	6.8	4.4	3.9
2. Loparskaya	68N	33E	+64	266		8.2	5.4	5.0	3.8
3. Sodankylä	67N	27E	+63	270	0.35	9.3	8.3	4.4	4.0
4. Lycksele	65N	19E	+62	271		6.6	5.1	4.8	3.9
5. Arkhangelsk	64N	40E	+59	268		12.0	8.0	5.9	4.0
6. Uppsala	60N	18E	+58	267		13.6	8.6	5.4	3.8
7. Leningrad	60N	30E	+56	269		12.2	7.7	5.5	3.7
8. Juliusruh	55N	13E	+54	270		14.8	9.6	5.3	3.9
9. Slough	52N	1W	+54	258	0.48	10.1	8.6	5.0	3.6
10. Moscow	56N	37E	+51	268	0.46	13.7	10.7	5.5	4.0
11. Wallops Is	38N	75W	+49	268	0.44	8.9	8.5	4.6	3.8
12. Wakkanai	38N	142E	+36	272	0.57	19.4	10.8	5.5	3.9
13. Norfolk Is	29S	168E	−37	282	0.45	29.2	6.9	1.8	3.7
14. Port Stanley	52S	58W	−41	261	0.61	39.9	10.4	1.3	3.5
15. Mundaring	32S	116E	−43	275	0.38	21.2	8.1	2.3	3.7
16. Kerguelen	49S	70E	−59	297	0.40	19.8	12.1	1.2	3.6
Mean of N. Hemisphere stations				268	0.46	12	8	5.1	3.8
Mean of S. Hemisphere stations				279	0.46	28	9	1.6	3.6
b									
1. Kiruna	68N	20E	+65	357		11.5	6.2	3.7	3.9
2. Loparskaya	68N	33E	+64	363		10.6	7.3	3.6	3.4
3. Sodankylä	67N	27E	+63	374	0.46	12.2	12.1	2.5	3.5
4. Lycksele	65N	19E	+62	373		9.4	7.2	3.5	3.5
5. Arkhangelsk	64N	40E	+59	362		10.1	8.8	2.7	3.5
6. Uppsala	60N	18E	+58	378		11.6	7.2	3.5	3.5
7. Leningrad	60N	30E	+56	373		11.9	8.5	2.7	3.6
8. Juliusruh	55N	13E	+54	379		9.0	8.5	3.4	3.8
9. Slough	52N	1W	+54	378	0.43	6.8	6.8	4.0	3.6
10. Moscow	56N	37E	+51	374	0.50	7.8	9.5	4.2	3.7
11. Wallops Is	38N	75W	+49	348	0.37	10.1	8.0	5.2	3.9
12. Wakkanai	38N	142E	+36	366	0.56	7.8	6.5	5.2	3.7
13. Norfolk Is	29S	168E	−37	340	0.38	17.2	6.1	2.2	3.1
14. Port Stanley	52S	58W	−41	387	0.55	8.6	7.9	3.6	4.0
15. Mundaring	32S	116E	−43	338	0.33	16.4	6.7	2.2	4.1
16. Kerguelen	49S	70E	−59	340	0.48	25.1	7.6	3.4	2.9
Mean of N. Hemisphere stations				369	0.46	10	8	3.7	3.6
Mean of S. Hemisphere stations				351	0.44	17	7	2.8	3.5

spring than in autumn. Table 1a, b gives values of the annual mean h_0 for $F_{10.7}$ = 140, which represents a midway value between solar minimum ($F_{10.7} \approx 70$) and the peak values of $F_{10.7}$ at the three solar maxima (232 in 1958, 156 in 1970, 203 in 1981 and 212 in 1989); 140 is also the value of $F_{10.7}$ used in the TIME-GCM runs (Sect. 3.1). The stations are arranged in order of decreasing magnetic latitude though, apart from Moscow and Port Stanley, the order would be unchanged if instead they were arranged geographically. The values of h_0 for the Northern Hemisphere stations are rather uniform, averaging 268 km by day and 369 km at night, with no clear latitude trend. The southern stations are less consistent, but on average hmF2 is higher by day (279 km) and lower at night (351 km) than in the Northern Hemisphere. The rate of increase with solar flux, $dh_0/dF_{10.7}$ (shown for a representative selection of stations), averages 0.44–0.46 km/unit by day and night in both hemispheres. As mentioned in Sect. 2.1, the values of $dh_0/dF_{10.7}$ may be a little too large, the overestimate being perhaps 0.05 km/unit.

2.3 Fourier analysis to derive annual and semiannual components

For the Fourier analysis, we take twelve monthly data values for a given year and fit mean, annual and semiannual components, thus:

$$h\text{mF2} = h_0 + h_1 \cos((\pi/6)(t - \phi_1))$$
$$+ h_2 \cos((\pi/3)(t - \phi_2)) \qquad (2)$$
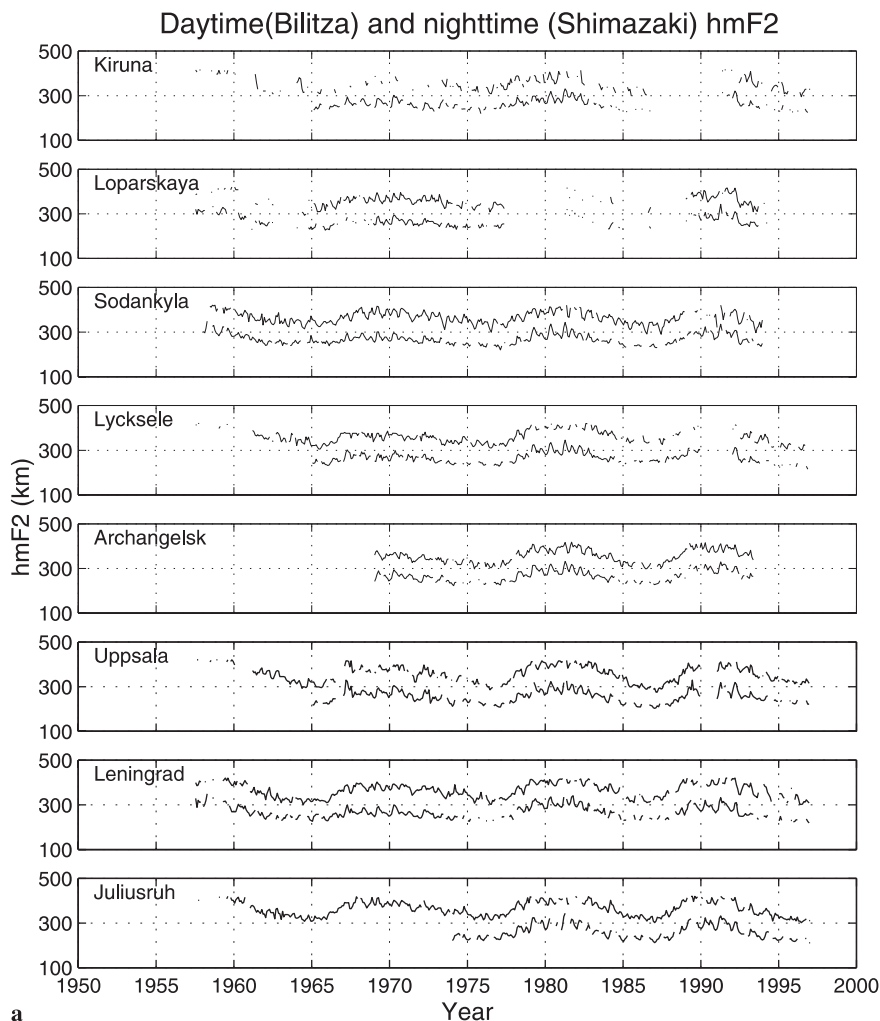
Fig. 2a, b. Time sequences of day (10–14 LT) (*lower curve in each box*) and night (22–02 LT) (*upper curve in each box*) values of *h*mF2, computed from tabulated MUF factors derived from ionograms, using monthly values for 16 stations arranged in order of decreasing magnetic latitude. **a** Kiruna to Juliusruh; **b** Slough to Kerguelen

where the amplitudes h_0, h_1, h_2 are in kilometres, and time t and the phases ϕ_1 and ϕ_2 are in months, zero phase being a maximum in mid-December. These phases, based on one-monthly data points, should be accurate to ½ month or possibly slightly better.

Figure 3 shows the importance of the "$M3000$ correction" ΔM for underlying ionization, using two stations with very good datasets, Moscow and Sodankylä. The upper boxes show the annual and semiannual amplitudes h_1 and h_2 for daytime, derived by using the "Bilitza formula", Eq. (1b), which includes the correction; the lower boxes show the corresponding results given by the plain "Shimazaki formula", Eq. (1a), which does not. Applying the correction ΔM clearly makes a great difference to the annual amplitudes, but has much less effect on the semiannual amplitudes.

The reason is not far to seek. If ΔM is omitted or is incorrect, the computed annual component in hmF2 is strongly influenced by the F1-layer, which is most prominent in summer and usually absent in winter, as well as by the E-layer. As the critical frequencies foE and foF1 are closely controlled by the solar zenith angle, which is the same at both equinoxes, variations of the E- and F1-layers should not seriously affect the semiannual component.

Figure 4 shows periodograms for five of the stations, chosen to give a wide geographical spread. It is obvious that the relative strength of the annual and semiannual components may be quite different between day and night at one station, and also that it varies greatly between stations. Compare, for example, the almost pure annual variation at Port Stanley (day) to the predominantly semiannual variation at Moscow (night). With a data run of 30 years, as available at most of these stations, the resolution is of order 3% (or 0.4 month) for the annual variation and 1.5% (or 0.1 month) for the semiannual variation. Tests made for Sodankylä, using the polynomial method of Titheridge (1969) to compute real heights, give similar results but with a rather smaller semiannual/annual ratio than shown in Fig. 3.

2.4 Annual and semiannual components: results

Figure 5a for day and 5b for night show the amplitudes h_0, h_1, h_2 plotted against the annual mean values of $F_{10.7}$ for the same five stations as used in Fig. 4, each point representing an individual year. The data points are well fitted by straight lines, with high correlation coefficients $r(h_0)$, both by day (0.81–0.94) and at night (0.75–0.92).
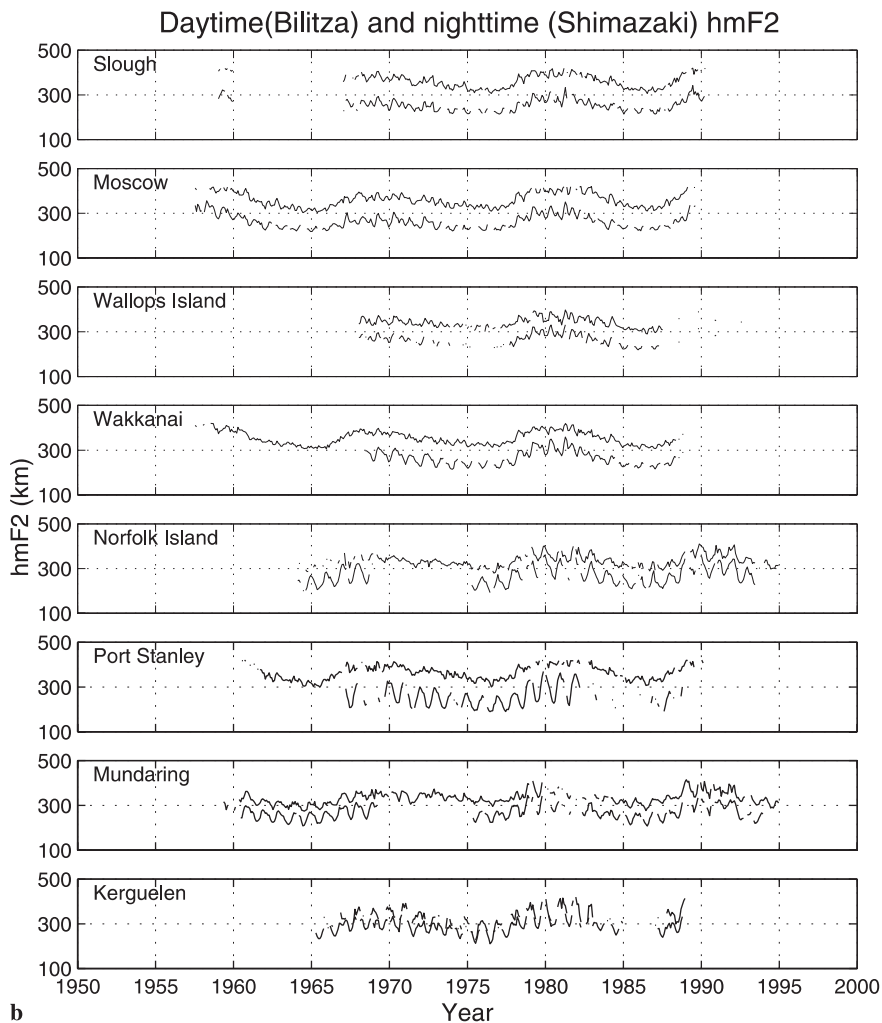
Daytime(Bilitza) and nighttime (Shimazaki) hmF2

Fig. 2b

b Year

The 5% significance levels (2 standard deviations) are in most cases ($\pm$) 20–30 km.

The centre and right-hand boxes in Fig. 5a, b show the plots of h_1 and h_2 versus $F_{10.7}$, also fitted with straight lines. These plots contain a great deal of scatter, but by day there is a clear upward trend. For northern stations the correlation coefficients $r(h_1)$ are in the range 0.35–0.8 and $r(h_2)$ are in the range 0.4–0.7, but the correlation coefficients are on the whole smaller at southern stations (0.07–0.5). The rates of increase are such that, from solar minimum ($F_{10.7} = 70$) to solar maximum ($F_{10.7} = 200$), daytime h_1 increases on average by 10 km and daytime h_2 by 8 km. At night the variations of h_1 and h_2 with $F_{10.7}$ are not significant; the correlation coefficients are small (mostly < 0.3) and most are negative, implying a slight tendency for the amplitudes to decrease with increasing $F_{10.7}$. Numerical values of h_0, h_1, h_2 at $F_{10.7} = 140$ for all sixteen stations are given in Table 1a for day and 1b for night.

Port Stanley stands out from the other stations because of its very large day-to-night change in h_0 and its large daytime annual component h_1, which doubles in amplitude from solar minimum (30 km) to solar maximum (60 km). The low daytime h_0, high nighttime h_0, and large daytime amplitude h_1 at Port Stanley is seen

also at number 14 in Fig. 6, which shows the Fourier results for all stations. A large daytime annual component h_1 is seen at the southern stations (13–16), and at Wakkanai in the Northern Hemisphere (12). Other notable features are the low daytime h_0 at Slough (9) and the low nighttime h_0 at Wallops Island (11).

As for phases, Table 1a shows that, at northern stations by day, the annual phase ϕ_1 is in the range 4–6 months, corresponding to maximum in mid-April to mid-June, and in late summer (1–2 months) at the southern stations (13–16). The semiannual phase ϕ_2 is consistently near equinox (3–4 months). At night, Table 1b shows that the semiannual variation again has its maxima near equinox, but the annual phase is usually earlier than by day, the maximum being at 2–5 months (February–May). We found no well-defined variation of the phases with $F_{10.7}$ though, at lower $F_{10.7}$, when the amplitudes are smaller and the phases are less well determined, there is more scatter, particularly in the annual component.

From the midlatitude results, in particular the consistent values of ϕ_2, we conclude that the semiannual variation of noon hmF2 is real. Its amplitude h_2 is rather smaller than the annual amplitude h_1. The combination of the semiannual spring maximum and the early summer
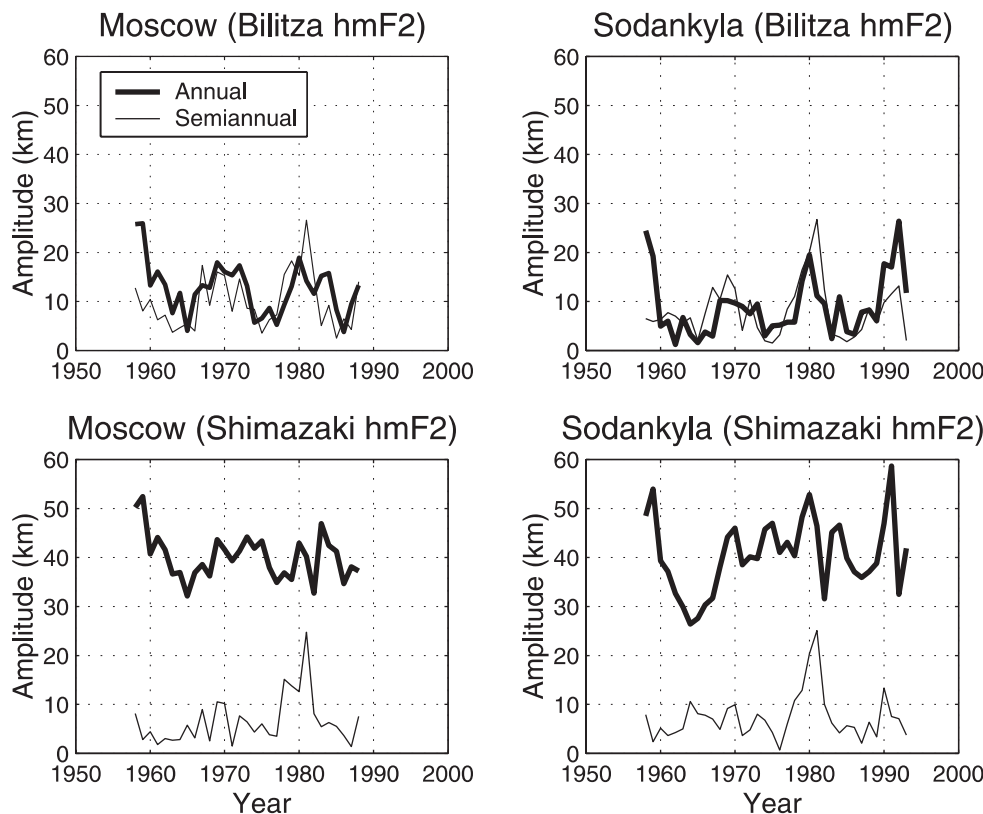
Fig. 3. Comparison of the amplitudes of the annual and semiannual components of hmF2, with ("*Bilitza*") and without ("*Shimazaki*") corrections for ionization underlying the F2-layer for day (10–14 LT)

maximum of the annual component produces an April or May maximum of noon hmF2 at northern stations; in the south, with a relatively small semiannual component, the maximum occurs in January or February.

2.5 Incoherent scatter data on hmF2 at Millstone Hill

We examined daytime values of hmF2 obtained in 1968–1971 from the incoherent scatter radar at Millstone Hill (43°N), given by Papagiannis *et al.* (1975) in the following form:

$$h\text{mF2} = 280 + 9K\text{p} = 304 \text{ [km] (summer)} \tag{3a}$$

$$h\text{mF2} = 290 + 4K\text{p} = 301 \text{ [km] (equinox)} \tag{3b}$$

$$h\text{mF2} = 265 + 5K\text{p} = 278 \text{ [km] (winter)} \tag{3c}$$

where the last value in each line is for Kp = 2.7, the mean value for the years in question. In this period the average $F_{10.7}$ is 144, so these values of hmF2 may reasonably be compared with the ionogram-derived values for $F_{10.7}$ = 140. Annual and semiannual amplitudes and phases cannot be determined from three values, but we can derive *minimum* amplitudes by assuming that the annual component maximizes in summer and the semiannual component at equinox. With these assumptions, the annual mean is 296 km, the annual amplitude is 13 km and the semiannual amplitude is 10 km, all of which are rather greater than the values derived from ionosonde data at northern stations (Table 1a). If the phases are not as assumed, the amplitudes will be greater.

3 Modelling of hmF2 with global thermosphere-ionosphere models

3.1 Global modelling using TIME-GCM

In Table 2 we show results obtained from the TIME-GCM Community Climate Model 3 for seven stations (which were chosen for another investigation, five of them being the same used in our data analysis); the values of hmF2 were kindly made available by R. G. Roble. For the simulation, solar activity is fixed at a moderate level ($F_{10.7}$ = 140 flux units) and magnetic conditions are quiet. We took smoothed daily values of hmF2 to represent day 16 of each month; the daytime results are for 12 LT, the nighttime results for 02 LT (which, for our purposes, does not differ significantly from midnight).

Table 2 shows that hmF2 is consistently higher in summer than in winter, both by day and by night. By day, the amplitude h_1 is larger in the Southern than in the Northern Hemisphere, but not necessarily at night. In all cases the annual maximum occurs in local summer. The semiannual variation is barely significant, the amplitude h_2 being small compared to h_1 at all the stations, so the semiannual phase is poorly determined. As TIME-GCM uses a height step of ½ scale height, corresponding to about 25 km, the fitting procedure used to derive hmF2 should be accurate to one-third of a height step, and thus better than 10 km, so the values of h_1 should be reliable even if those of h_2 are not. No relationship is found in the TIME-GCM results between the amplitudes of the semiannual variations of hmF2 and those of NmF2.
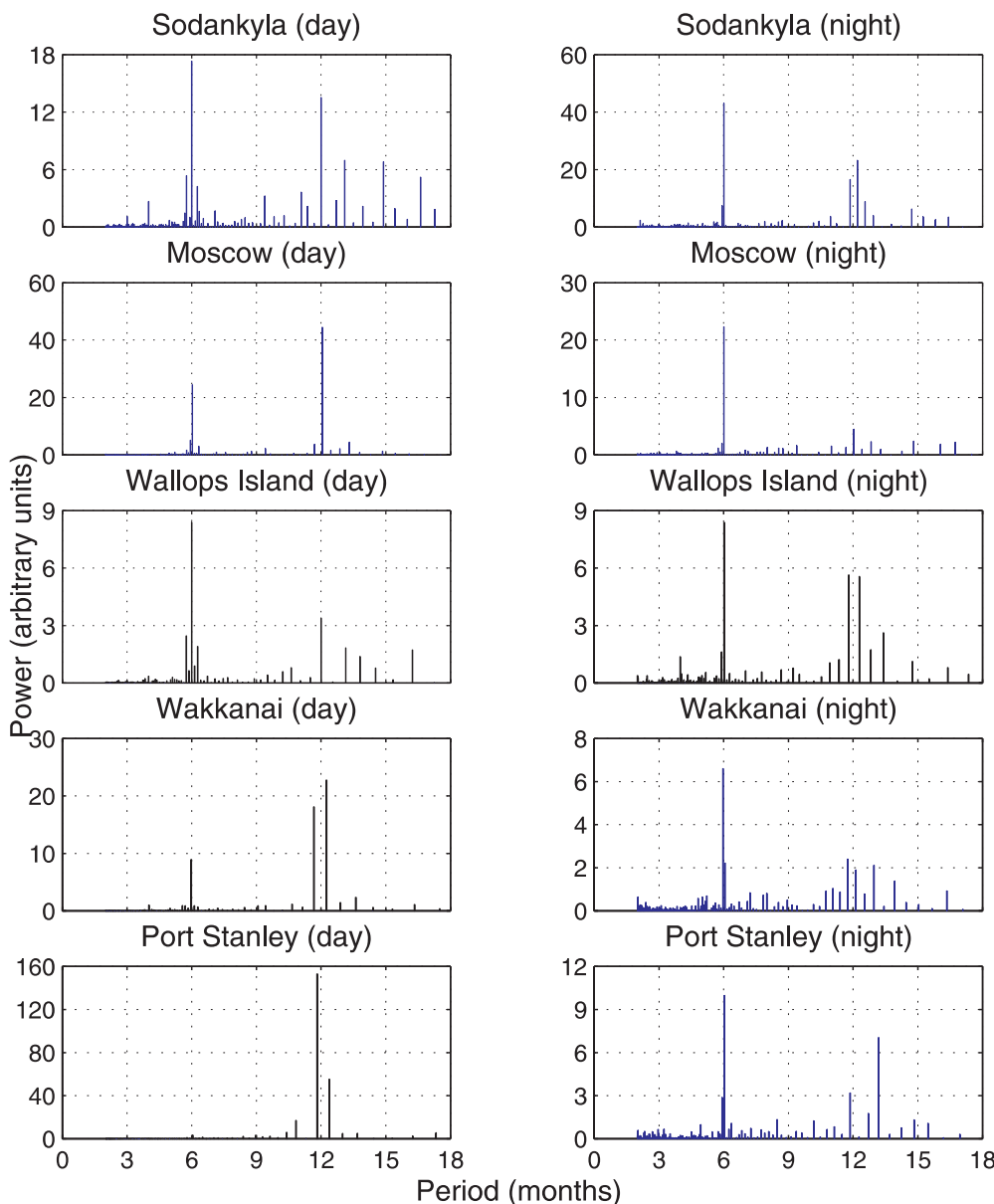
**Fig. 4.** Day (10–14 LT) and night (22–02 LT) periodograms of *h*mF2 for five stations

Table 2. Midday and night *h*mF2: amplitudes and phases from TIME-GCM model, $F_{10.7} = 140$

Station	Geographic		Noon 12 LT					Night 02 LT				
	Latitude (°)	Longitude (°)	Mean	Annual		Semiannual		Mean	Annual		Semiannual	
			h_0 (km)	h_1 (km)	ϕ_1 (mo)	h_2 (km)	ϕ_2 (mo)	h_0 (km)	h_1 (km)	ϕ_1 (mo)	h_2 (km)	ϕ_2 (mo)
Moscow	56N	37E	260	14	5.7	2	4	304	29	6.4	13	0
Slough	52N	1W	258	13	5.5	4	4	313	37	6.4	9	0
Wakkanai	45N	142E	263	19	5.1	5	1	300	39	6.0	5	0
Wallops Is	38N	75W	265	12	4.8	3	4	304	20	6.6	5	0
Port Stanley	52S	58W	259	30	0.3	8	4	352	47	0.1	12	1

3.2 Global modelling using CTIP

The CTIP model was run as described by Zou *et al.* (2000), for each month of the year, assuming constant solar activity of $F_{10.7} = 100$ units and quiet geomagnetic conditions ($K\mathrm{p} = 2$, $A\mathrm{p} = 7$). At noon, the mean level h_0 is about 260 km at high midlatitudes but, below magnetic latitudes $\pm 25°$, h_0 increases towards a value of about 360 km at the magnetic equator. With a computational height step of one scale height (typically 45 km),
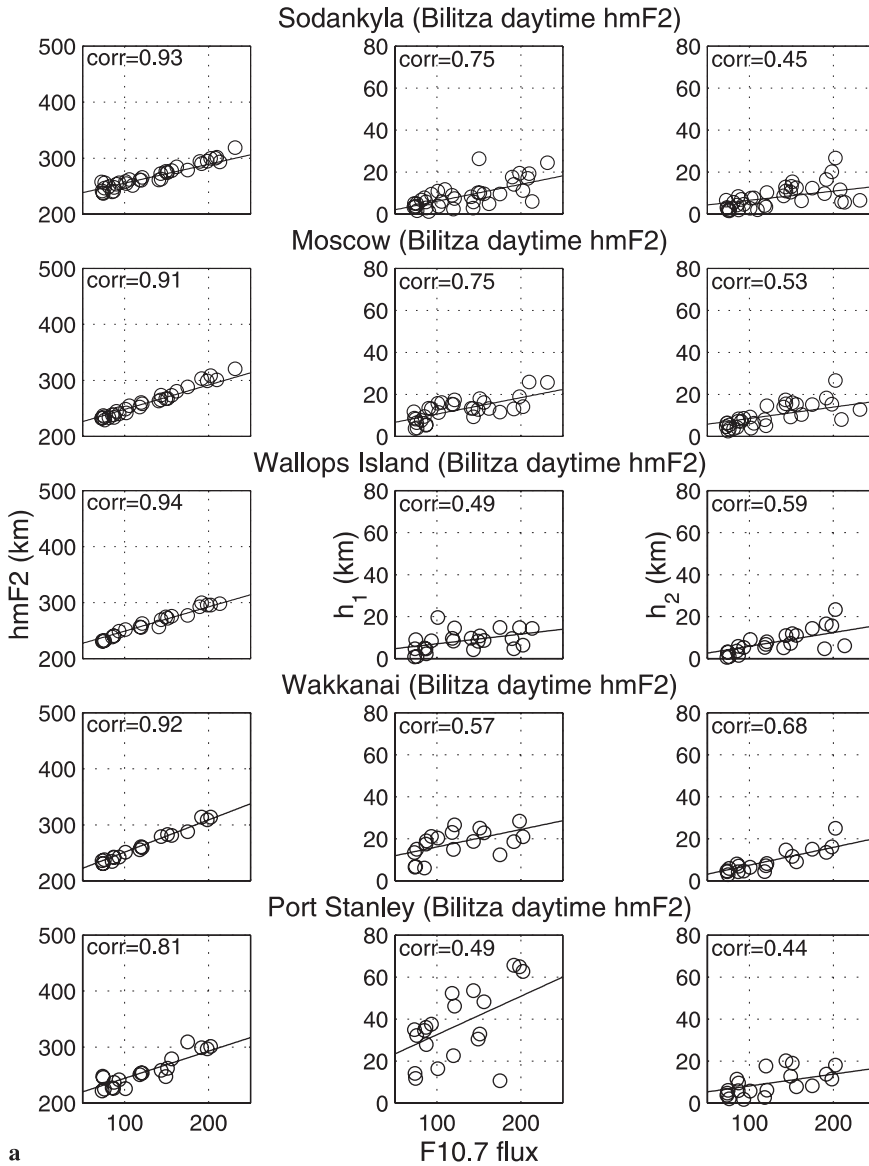
Fig. 5. a Annual means, annual and semi-annual amplitudes of hmF2, derived from ionograms, plotted versus 10.7 cm solar flux at five stations for day (10–14 LT). **b** Annual means, annual and semiannual ampitudes hmF2, derived from ionograms, plotted versus 10.7 cm solar flux at five stations for night (22–02 LT)

the accuracy of hmF2 is probably one-third of this, about 15 km, so the amplitudes are not very accurately defined. The phases are accurate to within 1 month.

Omitting the equatorial zone within magnetic latitudes $\pm 25°$, the Fourier components may be summarized as follows. At noon, the annual amplitude h_1 is about 15 km at northern midlatitudes. In the Southern Hemisphere h_1 varies with longitude, being about 15 km in western longitudes and 20–25 km in eastern longitudes. The phase ϕ_1 corresponds closely to summer solstice, i.e. 0–1 month in the southern magnetic hemisphere, 6 months in the north, the boundary being at the magnetic and not the geographic equator. The semiannual amplitude h_2 is very small (< 5 km) at midlatitudes, with phase $\phi_2 \approx 3$ corresponding to equinox. The results for midnight are broadly similar, except that the mean level is 310–360 km (varying with longitude); the semiannual component is slightly larger than by day, with $h_2 \leq 10$ km and maxima near solstice ($\phi_2 \approx 0$). The CTIP results for higher solar activity, $F_{10.7} = 180$, show a

similar distribution of annual and semiannual components, but with an amplitude ratio h_1/h_2 that is rather smaller (typically by about 30%) than at $F_{10.7} = 100$.

Comparing the CTIP and TIME-GCM results for the seven stations listed in Table 2, we find a great deal of similarity. Averaged over the seven stations, the mean values h_0 are about 5 km lower for CTIP than for TIME-GCM but about 12 km higher at night. The annual amplitude h_1 is in most cases smaller for CTIP than for TIME-GCM, notably at Port Stanley. The differences seem to be associated with the meridional winds, which are particularly strong in TIME-GCM in this sector, and are very dependent on the details of the neutral temperature and pressure distributions. The phase of the annual component of hmF2, with maximum in summer in both models, agrees with all the noon data and almost all the night data shown in Table 1a, b.

In both CTIP and TIME-GCM, most of the semiannual amplitudes h_2 are only a few kilometres which, being rather small compared with the corresponding h_1,
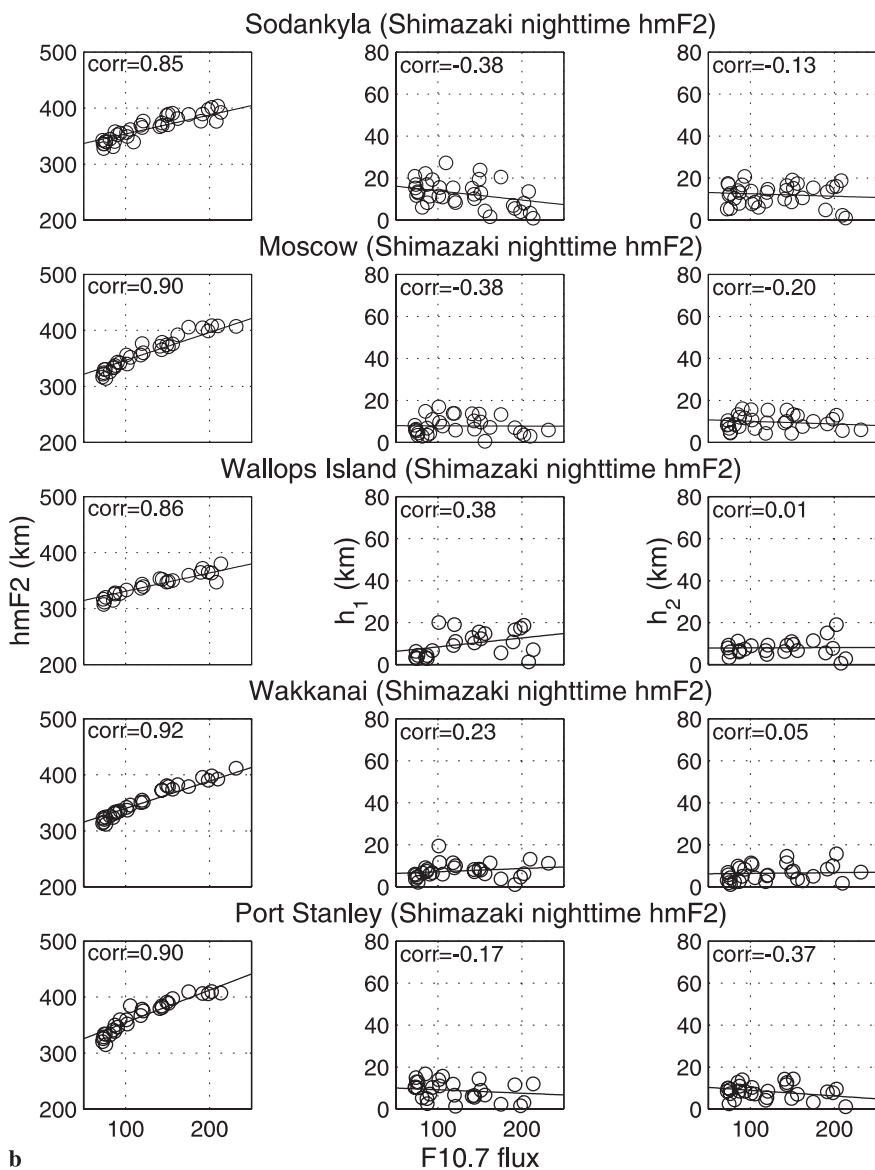
Fig. 5b

are not well determined by the analysis, nor are the derived phases ϕ_2 trustworthy. The important conclusions are that the CTIP and TIME-GCM results for hmF2 agree quite well, and that the semiannual components are much smaller than are found in the ionosonde data.

4 Semiannual variations in MSIS

According to Rishbeth and Edwards (1989), the F2-peak at a given local time should lie approximately at a constant pressure-level, for all seasons and all levels of solar activity. For midlatitude stations generally, these fixed pressure-levels are 20 μPa at noon and 2 μPa at midnight. We can test this assertion against the well-known MSIS (Mass Spectrometer/Incoherent Scatter) model, which is widely used to represent the behaviour of thermospheric parameters. To do this, we examine

how the heights h_{PD} and h_{PN} of the daytime and nighttime levels, defined by the pressure values just quoted, vary with season and solar activity, and compare them with the ionosonde values of hmF2. For this purpose we use the extended version MSISE-90 of Hedin (1991), although, since we consider only F-region heights between about 200 and 450 km, the extension below 90 km is not relevant to our study and for simplicity we use the term MSIS. As the nighttime TIME-GCM data used in Sect. 3.1 are for 02 LT instead of 00 LT (midnight), we use 02 LT for the MSIS study, which should make no significant difference.

4.1 Quiet-day MSIS data

We ran the MSIS model for the stations shown in Figs. 4 and 5, namely Sodankylä, Slough, Wakkanai, Wallops Island and Port Stanley. As the MSIS parameters vary
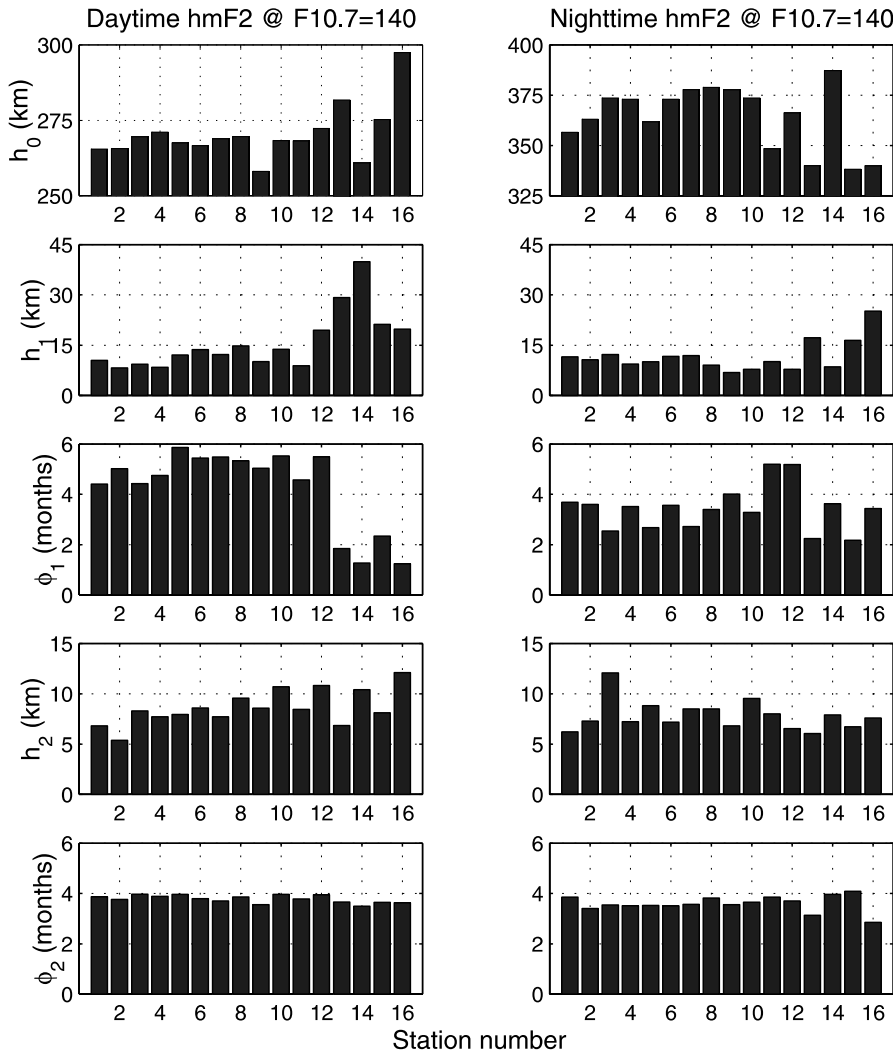
Fig. 6. Day and night values of annual mean hmF2 (h_0) and the amplitude and phase of the annual component (h_1, ϕ_1) and semiannual component (h_2, ϕ_2) for day (10–14 LT) and night (22–02 LT), solar 10.7 flux 140 units. The stations are arranged in *north*-to-*south* order of magnetic latitude (*1*, Kiruna, *2*, Loparskaya, *3*, Sodankylä, *4*, Lycksele, *5*, Arkhangelsk, *6*, Uppsala, *7*, Leningrad, *8*, Juliusruh, *9*, Slough, *10*, Moscow, *11*, Wallops Is, *12*, Wakkanai, *13*, Norfolk Is, *14*, Port Stanley, *15*, Mundaring, *16*, Kerguelen)

only slowly with latitude and longitude, the choice of locations is not critical, and it seemed unnecessary to do the calculations for all sixteen stations. We use the same two local times, 12 LT and 02 LT, and three levels of solar activity, $F_{10.7}$ = 70, 140 and 200. To test the effect of geomagnetic activity, we use two different conditions: "quiet", for which we take Ap = 3; and "average", for which we take Ap = 13, 17 and 20 to represent average conditions for the three levels of $F_{10.7}$. We further discuss the effect of varying Ap in Sect. 4.2.

In Fig. 7a for day and 7b for night, the MSIS pressure-level heights h_{PD} and h_{PN} are plotted against $F_{10.7}$, with circles denoting quiet and crosses denoting average magnetic conditions. Some numerical data are shown in Table 3. The annual mean values of h_{PD} and h_{PN} (tabulated for $F_{10.7}$ = 140) agree quite well with hmF2 (Table 1a, b). They do not vary much between stations, and neither do their rates of change with solar activity, which are $dh_{PD}/dF_{10.7} \approx 0.6$ km/unit and $dh_{PN}/dF_{10.7} \approx 0.9$ km/unit (averaged over the range $F_{10.7}$ = 70 to 200).There is some difference between day and night in that, as $F_{10.7}$ increases, the slope $dh_{PD}/dF_{10.7}$ increases slightly while $dh_{PN}/dF_{10.7}$ decreases, but these tendencies are too small to be easily seen in Fig. 7a, b.

The mean temperatures T at these pressure-levels, also shown in Table 3, vary from place to place, though not in the same way as the pressure-level heights, which depend on composition as well as on temperature. The mean rates of increase of temperature with $F_{10.7}$ are similar at all stations, about 3.7 K/unit for day and 2.9 K/unit for night, both decreasing with increasing $F_{10.7}$.

The phases of the semiannual variations of h_{PD} and h_{PN} are very consistent, namely 3.9 months, which corresponds to a maximum about 1 month after equinox. By day, the maximum of the annual component occurs near summer solstice, the phases being 6.0 months at the northern stations and 0.3 month at Port Stanley, though at night the annual phases are not consistent between stations.

The semiannual variations in MSIS agree very well in phase, and broadly agree in amplitude, with those derived from the ionosonde data (Table 1a, b). The annual variations disagree: in particular, the remarkably small daytime amplitudes at Wallops Island and Wakkanai have no counterpart in the ionosonde data (Table 1a) nor in the TIME-GCM simulations (Table 2). The nighttime MSIS amplitude at Sodankylä

Table 3. Temperatures (T), and the heights (h_P) and annual and semiannual variations of fixed pressure-levels derived from MSISE-90. The two bottom lines in each part of the Table show the variations with $F_{10.7}$ (not shown for the annual component because they vary considerably between stations). See text regarding phases

Station	Geographic latitude	Annual mean		Amplitude		$dh_P/dF_{10.7}$ (200-70) (km/unit)
		T (K)	h_P (km)	h_1 (km)	h_2 (km)	
20 µPa at 12 LT (h_{PD}) ($F_{10.7} = 140$, $Ap = 3$)						
Sodankylä	67N	1005	274	5	7	0.61
Slough	52N	1036	277	4	7	0.64
Wakkanai	45N	1058	278	1	7	0.63
Wallops Is	38N	1062	277	0.2	7	0.67
Port Stanley	52S	1020	276	14	6	0.62
Differences						
$F_{10.7}$: (140-70)		284	42	–	1.8	
$F_{10.7}$: (200-140)		200	38	–	1.7	
2 µPa at 02LT (h_{PN}) ($F_{10.7} = 140$, $Ap = 3$)						
Sodankylä	67N	938	370	3	11	0.92
Slough	52N	919	364	6	11	0.90
Wakkanai	45N	878	361	8	11	0.88
Wallops Is	38N	916	358	8	10	0.94
Port Stanley	52S	865	362	7	6	0.88
Differences						
$F_{10.7}$: (140-70)		231	64	–	1.8	
$F_{10.7}$: (200-140)		148	50	–	1.6	

is also small. Another obvious discrepancy is that the MSIS heights h_{PD} and h_{PN} increase more rapidly with increasing $F_{10.7}$ than do the F2-layer mean heights h_0.

4.2 How geomagnetic activity affects the annual and semiannual variations of pressure-levels

We now discuss the effect of geomagnetic activity, which peaks at the equinoxes (Fig. 1). Magnetic activity increases thermosphere temperature and density, so it raises the heights of fixed pressure-levels. Thus the seasonal variations of magnetic activity affect the annual and semiannual variations of hmF2. We cannot directly investigate this effect in our ionosonde data, because that would entail separating "quiet" and "disturbed" days, which would seriously reduce the quantity of usable hmF2 data. Nor do the TIME-GCM and CTIP simulations described in Sect. 3 shed any light on the matter, because they assume quiet conditions with low Ap. We can, however, estimate the "geomagnetic effect", i.e. how much the fixed pressure-levels h_{PD} and h_{PN} are raised when average levels of magnetic activity are put into the MSIS model.

For this purpose we use monthly mean values of Ap derived by M. Mendillo and colleagues (private communication, 1998) from geomagnetic data for 1955–1995, extracted from the CD-ROM produced by World Data Centre A for Solar-Terrestrial Physics. Three groups of years were defined according to the annual mean values of $F_{10.7}$, namely low ($F_{10.7} < 80$), medium ($140 < F_{10.7} < 155$) and high ($F_{10.7} > 175$), with mean values of Ap for "quiet" and "average" conditions as mentioned in Sect. 4.1. These groups correspond well to the levels $F_{10.7} = 70, 140, 200$ used for the MSIS runs.

We ran MSIS with the "average" values of Ap, and compared the heights h_{PD} and h_{PN} with those obtained from the "quiet" runs ($Ap = 3$). This enabled us to obtain the rates of change dh_{PD}/dAp for day (0.4–0.7 km/unit), and dh_{PN}/dAp for night (0.7–1.3 km/unit), as shown in Table 4. We now apply these results to annual and semiannual variations, making the simplifying assumption that h_{PD} and h_{PN} vary linearly with Ap, which seems reasonable for the moderate values of Ap involved. On average the temperature is 45 K higher at noon, and 63 K higher at night, for the "average" values of Ap than for the "quiet" values.

For "medium" solar activity ($F_{10.7} = 140$), the semiannual variation of Ap has amplitude $(Ap)_2 = 2.5$ units and phase 4 months (maximum 1 month after equinox). The annual variation is smaller, with amplitude $(Ap)_1 = 1.5$ units and phase also about 4 months. Because of its phase, the annual component of Ap is small at the solstices, its effect being to increase Ap at the March equinox and reduce it at the September equinox. (The amplitudes vary somewhat with $F_{10.7}$, and so does the annual phase; but we need not go into those details for our rough estimate of the geomagnetic effect.)

Combining the values of dh_{PD}/dAp and dh_{PN}/dAp with the amplitudes $(Ap)_1$ and $(Ap)_2$, we estimate the amplitude of the annual oscillations in h_{PD} and h_{PN} as shown in Table 4. The geomagnetic effect in the semiannual component is seen to be quite small, only 1–1.5 km by day and 2–3 km at night, and even smaller in the annual component. Comparing these with the semiannual amplitudes h_2 shown in Table 1, we conclude that the equinoctial peaks in geomagnetic activity
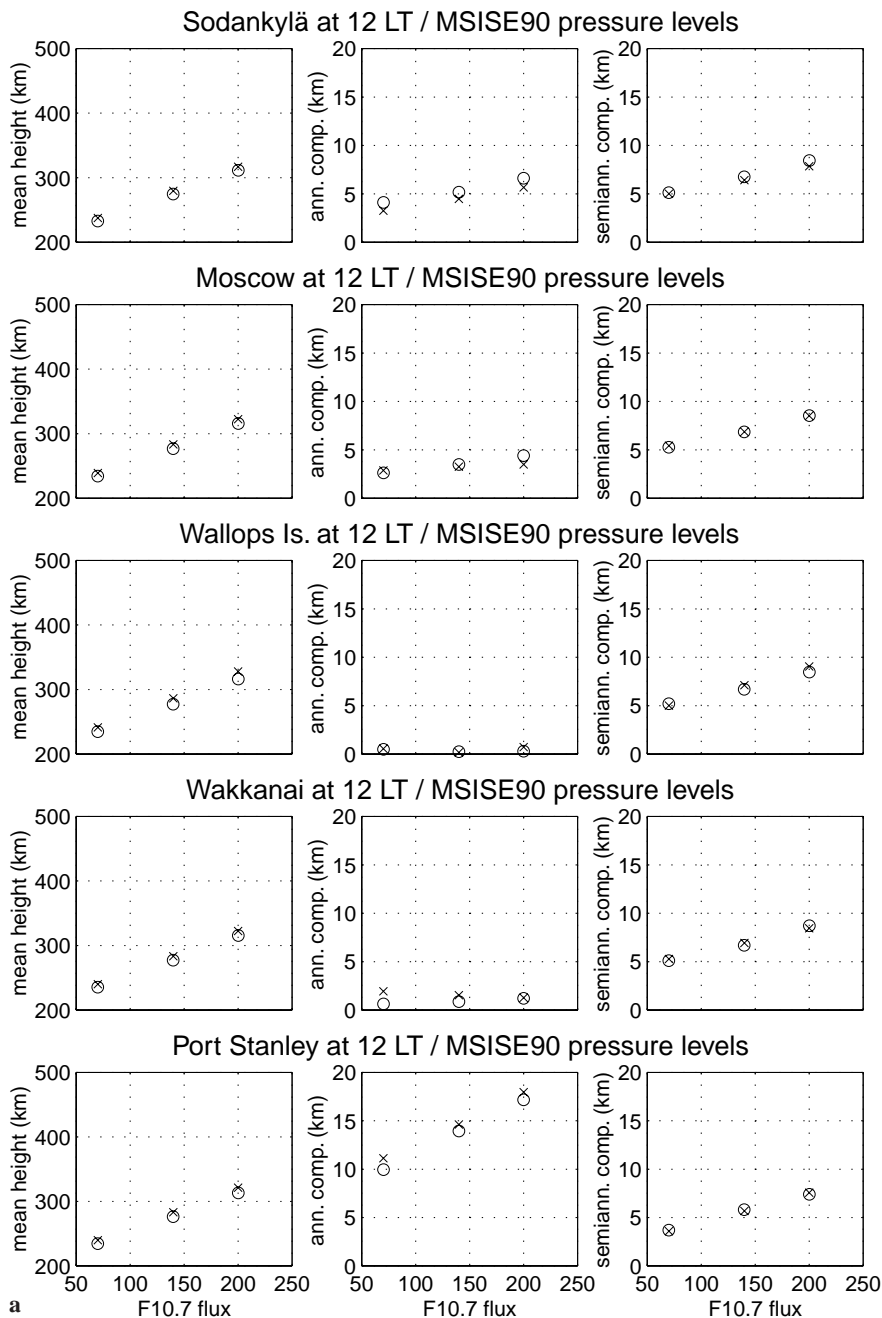
Fig. 7. a Annual means, annual and semi-annual amplitudes of the fixed pressure-level 20 μPa (approximately corresponding to daytime hmF2) plotted versus 10.7 cm solar flux at five stations for noon (12 LT). **b** Annual means, annual and semiannual amplitudes of the fixed pressure-level 2 μPa (approximately corresponding to nighttime hmF2) plotted versus 10.7 cm solar flux at five stations for night (02 LT)

cause only a minor part of the semiannual variation in hmF2. A similar conclusion may be drawn from the Millstone Hill data of Papagiannis *et al.* (1975) discussed in Sect. 2.5.

5 Discussion

The ionosonde data show that the semiannual variation in hmF2 is real. Its phase is consistent, with maxima shortly after equinox, and its amplitude increases with increasing $F_{10.7}$. At high $F_{10.7}$ the semiannual component is roughly equal to the annual component, which is fairly constant in phase (maximum in summer, minimum in winter), becoming earlier with increasing $F_{10.7}$.

The combination of the annual and semiannual components generally leads to a maximum of hmF2 in April or May in the north, and January or February in the south.

The southern stations (Port Stanley, particularly) and also Wakkanai show strong annual variations of hmF2 by day, which may be attributed to the seasonal variations of meridional winds. Wind effects are particularly strong at Port Stanley and Wakkanai, which are situated in longitudes remote from the magnetic poles (Rishbeth, 1998). At Port Stanley, the effect of strong diurnally varying winds is seen in the annual mean h_0; the night value of 387 km is the highest, and the day value of 261 km the second lowest, of any of the 16 stations. Furthermore, the magnetic dip angle I is close
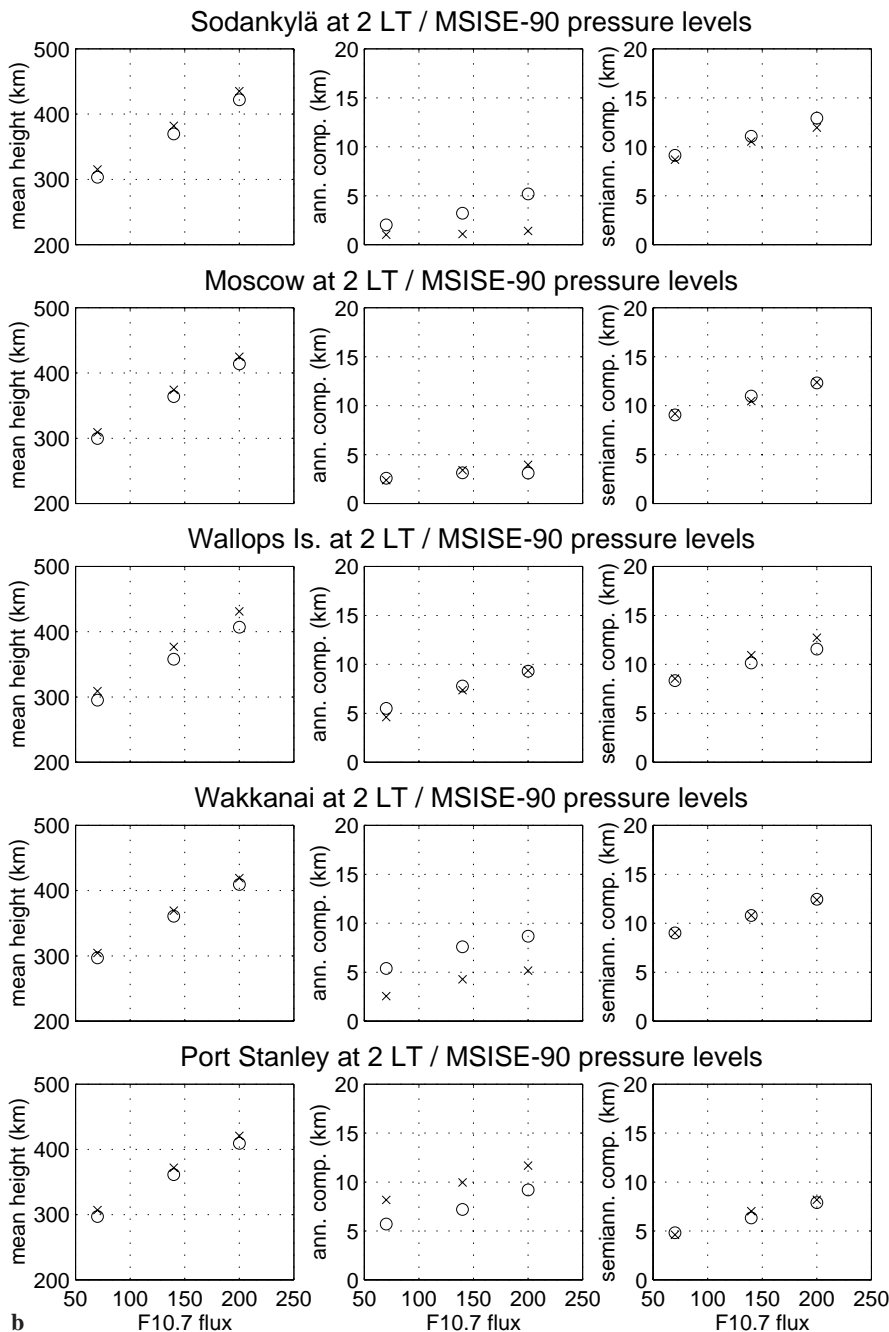
Fig. 7b

Table 4. Geomagnetic effect on the annual and semiannual variations of the heights of fixed pressure-levels (h_{PD} and h_{PN}) in the MSIS model, $F_{10.7} = 140$, assuming the annual amplitude of Ap to be $(A$p$)_1 = 1.5$ and the semiannual amplitude to be $(A$p$)_2 = 2.5$, as described in Sect. 4.2

Station	Geographic latitude	dh_P/dAp (km/unit)	h_P (annual) (km)	h_P (semiannual) (km)
12 LT Pressure-level (h_{PD})				
Sodankylä	67N	0.4	0.6	1.0
Slough	52N	0.7	1.1	1.8
Wakkanai	45N	0.6	0.9	1.5
Wallops Is	38N	0.6	0.9	1.5
Port Stanley	52S	0.7	1.1	1.8
02 LT Pressure-level (h_{PN})				
Sodankylä	67N	0.7	1.0	1.7
Slough	52N	1.2	1.8	3.0
Wakkanai	45N	0.9	1.4	2.3
Wallops Is	38N	1.3	1.9	3.2
Port Stanley	52S	1.0	1.5	2.5

to the value of 45° that maximizes the factor $\sin I \cos I$ (the vertical ion drift caused by a meridional wind U being given by $U \sin I \cos I$).

The annual mean of hmF2 increases with solar activity, on average by 0.45 km per unit of the flux $F_{10.7}$. The variation is not precisely linear, and is slower than the rise of constant pressure-levels with increasing $F_{10.7}$ as given by the MSIS model, about 0.6 km/unit at noon and 0.9 km/unit at night (Sect. 4.1). Over the range $F_{10.7} = 70$ to 200, the discrepancy amounts to about 20 km by day and 60 km at night. This means that, as solar activity increases, hmF2 is not accurately "isobaric", it does not precisely follow constant pressure-levels. As shown by Rishbeth and Edwards (1989), hmF2 is strongly influenced by meridional winds. As these winds vary with solar cycle, they may be the cause of the discrepancy between hmF2 and the pressure-level heights.

We find no relation between the semiannual variations of hmF2 and the well-known variations of noon NmF2. For example, Port Stanley has a mainly annual (summer/winter) variation of hmF2 and a strongly semiannual variation of NmF2. Northern stations like Slough, Moscow and Wallops Island have a predominantly annual (summer/winter) variation of NmF2, but their annual and semiannual variations of hmF2 are comparable in amplitude. These are particular examples of the more general situation shown in the maps of Torr and Torr (1973), namely, that noon NmF2 at midlatitudes has a predominantly seasonal (winter/summer) variation in longitudes close to the magnetic poles, but elsewhere the variation is predominantly semiannual. This difference in behaviour is reproduced by CTIP (Millward *et al.*, 1996b; Rishbeth, 1998). For hmF2, we found that the largest summer/winter variations occur in southern latitudes, most notably at Port Stanley, where the thermospheric wind effects are particularly strong.

Several theories exist as to the origin of the F2-layer semiannual variation. In order from the Sun outwards, they include:

1. A hypothesis that the Sun's EUV radiation varies with heliographic latitude (Burkard, 1951), combined with the semiannual variation of the Earth's heliographic latitude;
2. The known semiannual variation in geomagnetic activity, which is attributed to geometrical effects, such as the variation of solar wind parameters with heliographic latitude and the geometry of solar wind/ magnetosphere coupling;
3. Semiannual changes of temperature and composition generated internally within the thermosphere by dynamical and chemical processes;
4. Possible semiannual variations in influences transmitted to the thermosphere from the underlying mesosphere, such as tides and waves of various kinds.

Dismissing (1) because of the lack of any supporting evidence, we tested (2) as described in Sect. 4.2, and found that the semiannual variation of magnetic activity accounts for less than half the semiannual variation of midlatitude hmF2. In this analysis we took the Ap index to represent the geomagnetic effect, and used MSIS to model the variation with Ap of thermospheric temperature and pressure. So our conclusion depends on how well MSIS represents the geomagnetically disturbed thermosphere. One mechanism that might provide the link between geomagnetic activity and the global semiannual temperature variation is the "conduction mode" oscillation of the thermosphere (Walterscheid, 1982), which is forced by the semiannually varying Joule heating at high latitudes and is thus related to the Ap index, at least in principle. Chaman Lal (1992, 1998) postulates some additional solar wind influence on the thermosphere, apparently in addition to that which is represented by indices such as Ap, but its physical mechanism is not clear.

As for (3): the TIME-GCM and CTIP models take account of the internal processes in the thermosphere, driven by solar ionizing radiation and the *quiet-day* energy inputs from the magnetosphere and solar wind. Despite their success in reproducing both seasonal and semiannual variations of NmF2, these models, at least in the versions used here, do *not* reproduce the semiannual variations in quiet-day hmF2 (Sect. 3). The rough estimates made in Sect. 4.2 suggests that, even if the semiannual geomagnetic variation were included in these models, this conclusion would not change. Nor do we think it would change if we used real height $N(h)$ analysis instead of the MUF-based formula for calculating hmF2 (Sect. 2.3).

There remain tidal and wave inputs from the mesosphere and lower levels (4) which, together with (2), seem the best available explanation of the equinox maxima in hmF2. The tidal input to the thermosphere is estimated as 10^{10} W, as compared to the solar EUV input of order 10^{13} W, but *if* this tidal input is modulated semiannually, it may explain the semiannual variations of thermospheric temperature and thus of hmF2 (A. S. Rodger, private communication, 1998). Gravity wave inputs (e.g. Reid, 1986) also need to be considered.

6 Conclusions

At middle and low latitudes, we find that hmF2 has a well-defined relationship with solar activity, a clear annual variation (high in summer, low in winter), and a clear semiannual variation (high at equinox, low at solstice), comparable in amplitude to the annual variation. The semiannual variation of hmF2 is not related to that of NmF2, and is not reproduced by computational models of the quiet-day thermosphere and ionosphere (Sect. 3). Although our analysis uses both computational models (TIME-GCM and CTIP) and an empirical model (MSIS) to interpret the ionosonde data, we believe we have done this in a valid way.

Theory predicts that the height hmF2 depends on thermospheric density and temperature, so is affected by the semiannual variation in thermospheric density. On the assumption that hmF2 follows levels of constant atmospheric pressure (different for day and night), we find reasonably good agreement between the semiannual

component in the ionosonde hmF2 data and in the MSIS empirical mode (Sect. 4.1), and poor agreement in the annual component. The heights of the pressure-levels given by MSIS rise faster with increasing solar activity than do the values of hmF2. This discrepancy may be due to variations in meridional thermospheric winds.

Although hmF2 is affected by geomagnetic activity, which heats the thermosphere and thus raises the height of fixed pressure-levels, this accounts for only a small part of the observed semiannual variation of hmF2 (Sect. 4.2). For lack of another explanation, we suggest that the remainder is due to semiannually varying input of wave and tidal energy from lower levels in the atmosphere.

References

Bartels, J., Discussion of time variations of geomagnetic activity, indices Kp and Ap 1932–1961, *Ann. Geophysicae*, **19,** 1–20, 1963.

Becker, W., On the seasonal effect of the F-region at middle latitudes, in *Electron density distribution in ionosphere and exosphere*, Ed. E. Thrane, North-Holland, Amsterdam, 217–221, 1964.

Becker, W., The temperature of the F region deduced from electron number density profiles, *J. Geophys. Res.*, **72,** 2001–2006, 1967.

Bilitza, D., N. M. Sheikh, and R. Eyfrig, A global model for the height of the F2-peak using M3000 values from the CCIR numerical map, *Telecom. J.*, **46,** 549–553, 1979.

Burkard, O., Die halbjährige Periode der F2-Schicht-Ionisation, *Archiv Meteorol. Bioklim. Wien* **4,** 391–402, 1951.

Chaman Lal, Global F2 layer ionization and geomagnetic activity, *J. Geophys. Res.*, **97,** 12 153–12 159, 1992.

Chaman Lal, Solar wind and equinoctial maxima in geophysical phenomena, *J. Atmos. Solar-Terr. Phys.*, **60,** 1017–1024, 1998.

Dudeney, J. R., The accuracy of simple methods for determining the height of the maximum electron concentration of the F2-layer from scaled characteristics, *J. Atmos. Terr. Phys.*, **45,** 629–640, 1983.

Eccles D., J. W. King, R. Pratt, and H. Kohl, The semi-annual variation in the height of the F2-layer peak, *J. Atmos. Terr. Phys.*, **29,** 1641–1646, 1967.

Fuller-Rowell, T. J., D. Rees, S. Quegan, R. J. Moffett, M. V. Codrescu, and G. H. Millward, A coupled thermosphere-ionosphere model (CTIM), in *STEP handbook of ionospheric models*, Ed. R. W. Schunk, Utah State University, Logan, Utah, 217–238, 1996.

Green, C. A., The semiannual variation in the magnetic activity indices Aa and Ap, *Planet. Space Sci.*, **32,** 297–305, 1984.

Hedin, A. E., Extension of the MSIS thermospheric model into the middle and lower atmosphere, *J. Geophys. Res.*, **96,** 1159–1172, 1991.

McNamara, L. F., B. W. Reinisch, and J. S. Tang, Values of hmF2 deduced from automatically scaled ionograms, *Adv. Space Res.*, **7**(6), 53–56, 1987.

Millward, G. H., R. J. Moffett, S. Quegan, and T. J. Fuller-Rowell, A coupled thermosphere-ionosphere-plasmasphere model (CTIP), in *STEP handbook of ionospheric models*, Ed. R. W. Schunk, Utah State University, Logan, Utah, 239–280, 1996a.

Millward, G. H., H. Rishbeth, T. J. Fuller-Rowell, A. D. Aylward, S. Quegan, and R. J. Moffett, Ionospheric F2 layer seasonal and semiannual variations, *J. Geophys. Res.*, **101,** 5149–5156, 1996b.

Paetzold, H. K., and H. Zschörner, An annual and a semiannual variation of the upper air density, *Geofis. Pura Appl.*, **48,** 85–92, 1961.

Papagiannis, M. D., H. Hassan-Hosseinieh, and M. Mendillo, Changes in the ionospheric profile and the Faraday factor M with Kp, *Planet. Space Sci.*, **23,** 107–113, 1975.

Rawer, K., Synoptic ionospheric observations, including absorption, drifts and special programmes, *Ann. IQSY*, **5,** 97–130, 1969.

Reid, I. M., Gravity wave motions in the upper middle atmosphere (60–110 km), *J. Atmos. Terr. Phys.*, **48,** 1057–1072, 1986.

Rishbeth, H., How the thermospheric circulation affects the ionospheric F2-layer, *J. Atmos. Terr. Phys.*, **60,** 1385–1402, 1998.

Rishbeth, H., and R. Edwards, The isobaric F2-layer, *J. Atmos. Terr. Phys.*, **53,** 321–338, 1989.

Roble, R. G., E. C. Ridley, A. D. Richmond, and R. E. Dickinson, A coupled thermosphere/ionosphere general circulation model, *Geophys. Res. Lett.*, **15,** 1325–1328, 1988.

Shimazaki, T., World-wide variations in the height of the maximum electron density of the ionospheric F2 layer, *J. Radio Res. Labs.* **2**(7), 85–97, 1955.

Titheridge, J. E., Single-polynomial analysis of ionograms, *Radio Sci.*, **4,** 41–51, 1969.

Torr, M. R., and D. G. Torr, The seasonal behaviour of the F2-layer of the ionosphere, *J. Atmos. Terr. Phys.*, **35,** 2237–2251, 1973.

Ulich, T., and E. Turunen, Evidence for long-term cooling of the upper atmosphere in ionosonde data, *Geophys. Res. Lett.*, **24,** 1103–1106, 1997.

Walterscheid, R. L., The semiannual oscillation in the thermosphere as a conduction mode, *J. Geophys. Res.*, **87,** 10527–10535, 1982.

Yonezawa, T., The solar-activity and latitudinal characteristics of the seasonal, non-seasonal and semi-annual variations in the peak electron densities of the F2-layer at noon and at midnight in middle and low latitudes, *J. Atmos. Terr. Phys.*, **33,** 889–907, 1971.

Yonezawa, T., and Y. Arima, On the seasonal and non-seasonal annual variations and the semi-annual variation in the noon and midnight electron densities of the F2 layer in middle latitudes, *J. Radio Res. Labs.*, **6,** 293–309, 1959.

Zou, L., H. Rishbeth, I. C. F. Müller-Wodarg, A. D. Aylward, G. H. Millward, T. J. Fuller-Rowell, D. W. Idenden, and R. J. Moffett, Annual and semiannual variations in the ionospheric F2-layer. 1: A modelling study, *Ann. Geophysicae*, in press, 2000.